SCIENTIFIC REPORTS

OPEN

SUBJECT AREAS:
NANOPHOTONICS AND PLASMONICS
ULTRAFAST PHOTONICS
NONLINEAR OPTICS

Received
23 July 2014

Accepted
20 November 2014

Published
12 January 2015

Correspondence and requests for materials should be addressed to P.D. (dombi.peter@wigner.mta.hu)

* These authors contributed equally to this work.

Strong-field plasmonic photoemission in the mid-IR at <1 GW/cm^2 intensity

S. M. Teichmann[1]*, P. Rácz[2]*, M. F. Ciappina[3], J. A. Pérez-Hernández[4], A. Thai[1], J. Fekete[2], A. Y. Elezzabi[5], L. Veisz[3], J. Biegert[1,6] & P. Dombi[2]

[1]ICFO–Institut de Ciències Fotòniques, Mediterranean Technology Park, 08860 Castelldefels, Barcelona, Spain, [2]MTA ''Lendület'' Ultrafast Nanooptics Group, Wigner Research Centre for Physics, Konkoly-Thege M. út 29-33, 1121 Budapest, Hungary, [3]Max-Planck-Institut für Quantenoptik, Hans-Kopfermann-Str. 1, 85748 Garching, Germany, [4]Centro de Láseres Pulsados (CLPU), Parque Científico, 37185 Villamayor, Salamanca, Spain, [5]University of Alberta, Department of Electrical and Computer Engineering, T6G 2V4 Edmonton, Alberta, Canada, [6]ICREA–Institució Catalana de Recerca i Estudis Avançats, 08010 Barcelona, Spain.

We investigated nonlinear photoemission from plasmonic films with femtosecond, mid-infrared pulses at 3.1 μm wavelength. Transition between regimes of multi-photon-induced and tunneling emission is demonstrated at an unprecedentedly low intensity of <1 GW/cm^2. Thereby, strong-field nanophysics can be accessed at extremely low intensities by exploiting nanoscale plasmonic field confinement, enhancement and ponderomotive wavelength scaling at the same time. Results agree well with quantum mechanical modelling. Our scheme demonstrates an alternative paradigm and regime in strong-field physics.

The physics of strong-field laser-matter interaction has been, so far, within the domain of high-intensity (terawatt or multi-gigawatt) lasers. Nanolocalized electromagnetic fields in the vicinity of metallic structures are particularly suitable for inducing strong-field interactions of various materials with ultrashort laser pulses of lower energy. The electromagnetic field of a laser beam can be confined to nanometric dimensions with the help of various metallic structures along either one or all spatial coordinates. Plasmonic thin films[1–7] and plasmonic nanoparticles[8–10] as well as nanotips (which typically do not exhibit surface plasmon resonances)[11–13] are all suitable media for this purpose. The high degree of localization of the laser field in the vicinity of plasmonic metal structures inherently results in the well-known electric field enhancement phenomenon[14] that can amount to factors of several hundreds[15]. This feature was exploited only in recent years to access the realm of fundamental, strong-field physical light-matter interactions with low-energy laser pulses from femtosecond oscillators[6,7,10,16,17]. Related research includes the enhancement of extreme ultraviolet fluorescence with nanoparticles[16], and the observation of strong-field plasmonic photoemission both for propagating[6,7] and for localized surface plasmons[8–10]. In addition, the discovery of electron quiver motion quenching in nanolocalized electric fields[12] was made possible by high field localization.

The transition from perturbative to strong-field light-matter interactions can be characterized by the Keldysh parameter $\gamma = \sqrt{I_p/2U_p}$[18,19]. Here, I_p is the ionization energy of a given material and U_p is the ponderomotive energy of electrons (average kinetic energy of electrons in the oscillatory laser field) given by

$$U_p = \frac{e^2\lambda^2 E^2}{16\pi^2 m_e c^2}, \quad (1)$$

(where e is the electron charge, m_e is the electron mass, λ, E, and c are the wavelength, field strength amplitude, and speed of the light, respectively). In the strong-field regime, in which $\gamma \leq 1$, the ponderomotive energy becomes comparable to the electron binding energy. This regime requires typically focused laser intensities of 10^{14} W/cm^2 at 800 nm central wavelength. However, it was possible to achieve strong-field interactions at orders of magnitude lower focused intensities (40–60 GW/cm^2) by making use of nanoparticle field localization at the same wavelength[6,7,10].

This raises the fundamental question of what the lowest intensity is to observe strong-field phenomena and the corresponding electron kinetics. Eq. (1) and the considerations above tell us that one can exploit several physical phenomena at the same time. The favourable inverse scaling of the Keldysh-γ parameter with wavelength prompts us to use long-wavelength sources, possibly even in the THz region. On the other hand, we need to

restrict these studies for femtosecond sources where high enough intensities can be attained and this leaves us with the mid-infrared domain where recent developments enabled the generation of energetic femtosecond pulses with high repetition rates based on optical parametric amplification. To achieve strong-field interactions with low laser intensities, we also need to exploit plasmonic field enhancement, known to be significantly higher than the enhancement provided by the tip effect (cf. Refs. 14–17). In addition, as compared to typical 800 nm sources, we expect plasmonic field enhancement to be higher in the mid-infrared (e.g. ×14 for a propagating surface plasmon on a thin metal film for 800 nm wavelength and ×19 for 3.1 μm[14]). All in all, by employing mid-infrared lasers representing a compromise between available femtosecond sources and the drive for ever longer wavelengths, we can hope to achieve strong-field interactions at orders of magnitude lower intensities than in our previous studies where only standard 800 nm, Ti:sapphire lasers were used[6,7].

In this work, we show that the transition between multi-photon induced (perturbative) and strong-field light-solid interactions can be shifted to unprecedentedly low focused intensities of below 1 GW/cm^2 with the help of ultrashort, mid-infrared pulses and nanoplasmonic field confinement. In addition, we demonstrate that even at such low intensities, electron energies can be generated in a nanoscale plasmonic acceleration process that exceed the photon energy of the exciting pulse by almost two orders of magnitude. Accessing the strong-field realm at unprecedentedly low intensities is enabled by the simultaneous usage of a mid-infrared femtosecond source and exploiting *i)* the $1/\lambda-$scaling of the Keldysh-parameter and *ii)* the λ^2-scaling of the ponderomotive energy of the electrons, respectively.

Our concept and the corresponding scalings are illustrated in Fig. 1 showing some representative, numerically calculated trajectories of electrons, photoemitted into the field of a propagating surface plasmon[20,21]. Even though this illustration performed by the classical tracking of electron trajectories can not capture the quantum mechanical complexity of the process under scrutiny, it can well illustrate both the experimental geometry and the favourable ponderomotive electron acceleration behaviour when using mid-infrared light. In our experiments, coupling of the fundamental beam to surface plasmons was carried out in the Kretschmann-Raether coupling geometry[14] by using a right-angle prism, see Fig. 1(a). The electron trajectories following plasmonic photoemission induced by 800 nm light show small-amplitude oscillations and low electron energies (Fig. 1(b)), whereas surface plasmons induced by 3 μm light (Fig. 1(c)) wiggle the electrons significantly more with one order of magnitude higher final kinetic energy. This simple initial model calculation illustrates the viability of our concept. In the rest of our paper, however, we will rather use a different, full quantum mechanical simulation to model concrete experimental results.

Results

For our experiments, we used a state-of-the-art mid-infrared optical parametric chirped pulse amplifier (OPCPA) source[22] delivering 90 fs pulses at a central wavelength of 3.1 μm. These pulses were focused onto the hypotenuse face of a right-angle CaF_2 prism where they generated propagating surface plasmons on a 15 nm thick gold film. Plasmonic photocurrent and surface plasmon enhanced photoemission spectra were then measured with a retarding grid analyzer followed by an electron multiplier. Two independent measurements of the intensity dependence of the plasmonic photocurrent, excited by femtosecond laser pulses at 3.1 μm, are depicted in Fig. 2 on a double logarithmic scale. Intensity changes were controlled by varying the pump power of the last amplifier stage in the OPCPA. We confirmed that this procedure did not lead to modifications of the temporal profile of the pulse. The curves in Fig. 2 show that the total photocurrent first scales highly nonlinearly with the intensity (according to a ~13th power law), as expected from multi-photon induced photoemission with a photon energy of 0.4 eV and a work function of ~5.1 eV for polycrystalline gold. This behavior substantially changes at around 0.6 GW/cm^2 focused intensity where the local slopes of the curves are drastically reduced. This is a well-known signature of the photoemission mechanism changing into tunneling[6,7,23–25], however, in our case the transition takes place at unprecedentedly low intensities, suggesting a strong field enhancement related with the excitation of surface plasmons.

In order to determine the magnitude of the field enhancement responsible for this tunneling transition, we also measured the electron spectra for a variety of incident laser intensities and evaluated their cutoff point, as shown in Fig. 3(a). One can see that whereas the ponderomotive energy of electrons according to Eq. (1) is only between 1.3 and 3.1 meV for the incident laser intensities in

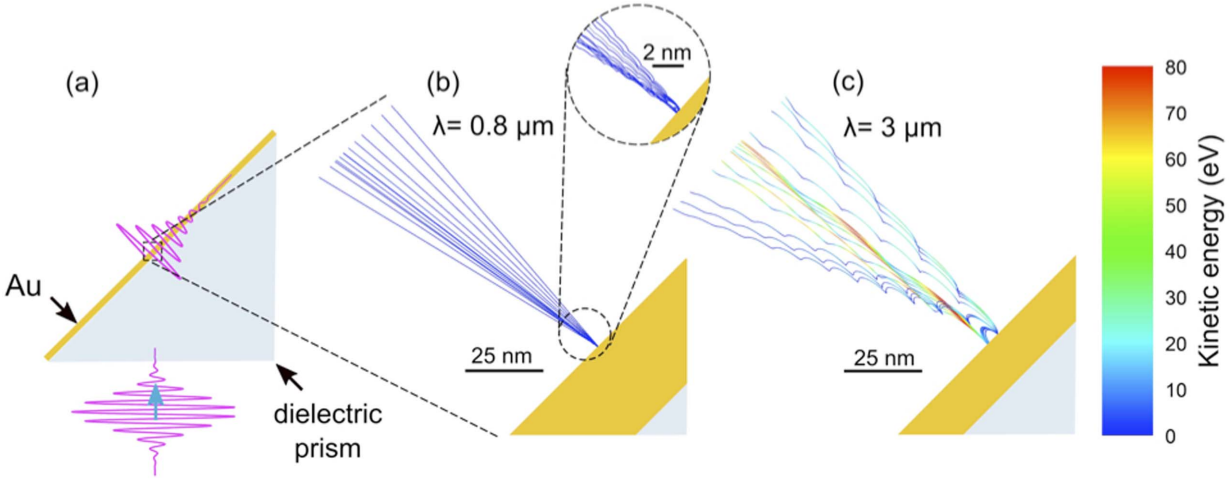

Figure 1 | Illustration of the concept of strong-field photoemission and electron acceleration in nanolocalized surface plasmon fields generated on thin gold films by focusing 9-cycle laser pulses in the Kretschmann-Raether coupling geometry (a). The advantage of using a long-wavelength mid-infrared femtosecond source is evident by depicting electron trajectories for surface plasmon excitation at (b) 800 nm central wavelength, 4 GW/cm^2 focused intensity and 24-fs FWHM pulses (~9 optical cycles) and (c) 3 μm central wavelength, 4 GW/cm^2 focused intensity and 90-fs FWHM pulses (~9 optical cycles). It can be seen that both the electron quiver amplitudes and the achievable kinetic energies are substantially increased in the long-wavelength case, in accordance with fundamental, ponderomotive scaling laws.

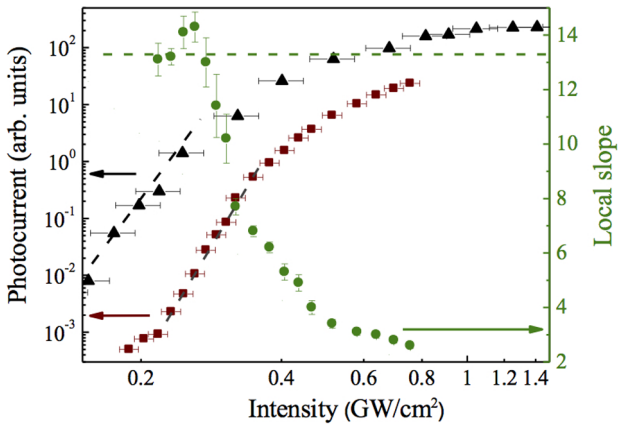

Figure 2 | Focused laser intensity dependence of the total plasmonic photocurrent for two independent exemplary scans (offset for clarity, black triangles and red squares). Spot sizes (FWHM) of 870 μm (black triangles) and 1400 μm (red squares) were used and the pulse energy was varied as described in the main text. The slopes of the fits to the initial sections (dashed lines) are 12.3 ± 1.8 and 13.1 ± 0.6, respectively. The local slope of the second curve is also plotted (green circles) to illustrate the gradual transition between multi-photon-induced and tunneling (strong-field) photoemission at very low laser intensities. The electron multiplier gain of each measurement was set such that for the maximum intensity the signal did not show a saturated trace on an oscilloscope. After that, quantitative voltage signal was acquired with a lock-in amplifier.

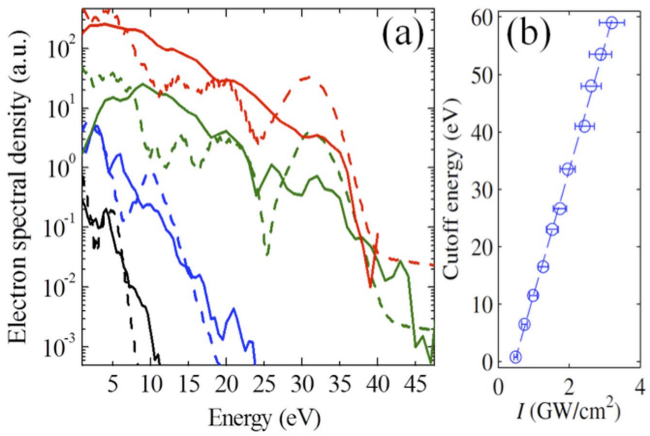

Figure 3 | (a) Plasmonic photoemission electron spectra for intensities 1.4 GW/cm² (black), 1.7 GW/cm² (blue), 2.8 GW/cm² (green) and 3.5 GW/cm² (red) in the strong-field photoemission regime. The evaluated plasmonic field enhancement factors are between 28 and 34. Dashed lines show the spectra calculated from the quantum mechanical model involving a plasmonic field enhancement factor (see main text). Note that the respective spectra are offset along the *y* axis for clarity. (b) Maximum kinetic energy of plasmonically accelerated photoelectrons as a function of focused laser intensity in an independent measurement. For a given intensity we increased the retardation field until the noise level was reached, being equivalent to the signal without any beam incident on the prism. The linear dependence of cutoff on intensity confirms the classical ponderomotive scaling law. All measurements were carried out with a spot size (FWHM) of 870 μm and the pulse energy was varied as described in the main text.

Fig. 3(a), orders of magnitude higher electron energies can be achieved in the surface plasmon field. Analyzing maximum kinetic energies of the spectra, i.e. the cutoffs, we find cutoff values of up to 47 eV.

We also carried out independent measurements of the maximum (cutoff) kinetic energy of the electrons as a function of intensity, without resolving electron spectra, by increasing the retardation field and monitoring the voltage where the electron multiplier signal reached the noise level. Results (shown in Fig. 3(b)) confirm that the electron acceleration process in the enhanced surface plasmon field is governed by the classical ponderomotive scaling law. According to Eq. (1), the maximum kinetic energy of electrons should be proportional to $I\lambda^2$ and this linear scaling with the intensity is observed clearly in the same intensity range as that of Fig. 2. Since the acceleration process is independent of the photoemission mechanism, a linear intensity dependence is observed irrespective of the multiphoton or strong-field nature of the emission process. As an additional confirmation of the validity of this interpretation, we investigated potential space charge effects numerically that could occur for our experimental parameters. We found that it is only from 10^5 electrons/shot that space charge effects distort the measured electron spectra and we are clearly below this value. Even for the highest intensities used in our experiments, the total number of photoemitted electrons per laser shot is estimated to be around 3000. Details of this simulation can be found as a Supplemental Material.

Discussion

The experimentally determined cutoff values (see Fig. 3(a)) allow us to approximately determine the maximum field enhancement factor at the evaporated thin film surface in the following way. It is known that the highest energy electrons undergo rescattering on the surface after a fraction of the light oscillation cycle[10,25–27]. Provided that the emission and rescattering events take place at the most favorable phases of the oscillating electromagnetic field, the electron can gain a kinetic energy amounting to as much as ten times the ponderomotive potential[26,27] if the electron quiver amplitude is smaller than the field decay length[12] which holds in our case as shown above. Therefore, by evaluating the cutoff points of the measured spectra, we can determine the maximum value of the ponderomotive potential within the focal spot by using the well-known $10 \times U_p$ cutoff law[26,27]. This cutoff law is universally valid irrespective of the medium, *i.e.* atom, surface, etc., and thus it is applicable to our case, too. It can be derived classically by considering the motion of an electron in the oscillating electric field of a laser pulse[26,27]. Depending on the instant of ionization relative to the peak of the electric field, the electron either does not return to its origin at all, returns only once or returns multiple times. In all cases, the electron gains kinetic energy from the electric field which we express in terms of the ponderomotive energy U_p in Eq. (1). If the electron does not return, its maximum kinetic energy can be shown to be about $2 \times U_p$ whilst this value increases to about $3.2 \times U_p$ at the first return[28,29] due to the additional time spent in the electric field. Upon the first return, the electron may elastically rescatter off the surface after which it gains additional kinetic energy from the electric field due to the favourable phase jump in the acceleration field. Clearly, this additional energy depends on the scattering angle Θ and the classical numerical analysis of the process reveals that if $\Theta = \pi$ relative to the initial direction of motion, the final kinetic energy amounts to a maximum of $10 \times U_p$. Since rescattering takes place in less than the half cycle time of the field and this initial phase of electron motion takes place within the closest nanoscale proximity of the surface (see e.g. Fig. 1), we can approximately measure the highest plasmonic field enhancement factor experimentally.

Carrying out this analysis with the measured cutoff values (see Fig. 3(a)), we find an increase of the cutoff by three orders of magnitude compared to the values expected from the focused intensities (see Eq. (1)) and the mentioned $10 \times U_p$ cutoff law. This finding corroborates a high effective field enhancement factor provided by the plasmonic thin film. In fact, the cutoff increase corresponds to field enhancement factors between 28 and 37 for the analysed spectra. We note that the maximum field enhancement factor of a

perfectly flat gold film with the 15 nm (resonant) thickness is 19 at this wavelength[14]. We attribute the somewhat higher measured values to additional surface roughness of the plasmonic film[6,7]. Thus, the large enhancement factor in combination with the $1/\lambda$ −scaling of γ allow for the generation of surface-confined electric fields sufficient for strong-field photoemission at focused laser intensities of only around 1 GW/cm^2.

Furthermore, to confirm our conclusions from a theoretical point-of-view, we carried out a quantum mechanical analysis of the strong-field light-matter interaction the results of which are also shown in Fig. 3(a). The theoretical model we used has already been described and employed for the calculation of the electron photoemission from metal nanotips[30]. See the Methods section for a brief overview.

To match the cutoff energies of a given experimental electron spectrum, we use the experimental intensity and vary the field enhancement factor in the simulation, representing the only fit parameter in our case. In each spectrum, the modelled cutoff corresponds to the discussed kinetic energy of $10\times U_p$, taking into account the field enhancement factor in determining the pondermotive energy. The parameters used for the model spectra plotted in Fig. 3(a) agree to within a factor of two with the experimentally determined enhancement factors. Best-match modelled electron spectra in Fig. 3(a) yielded field enhancement factors of between 60 and 70, representing higher enhancement values than those gained by the cutoff evaluation of measured spectra. This is, however, a satisfactory agreement on the magnitude of the field enhancement in this particular configuration taking into account the one dimensional nature of our quantum mechanical model and that we did not solve the plasmonic field distribution along the simulation grid with classical Maxwell solvers, but used a universal plasmonic field enhancement factor in the quantum mechanical model.

As discussed in Ref. 30, the model used is not able to reproduce the experiments exactly in the "direct" part of the photoelectron spectrum, i.e. the electron energy region less than $2 \times U_p$, due to the fact that a more detailed description of both the surface and the scattering potentials would be necessary. As a consequence, more pronounced peaks and dips appeared in our modelled spectra. In spite of this, the 1D model reproduces the cut-off (maximum energy) region reasonably well and this is so because we have put special emphasis on including the recollision phenomenon in our approach. We should stress, however, that more sophisticated approaches show similar features as the ones present in our model[31].

In conclusion, we demonstrated that with the help of nanoplasmonic field enhancement and long excitation wavelengths one can achieve strong-field light-matter interaction at unprecedentedly low incident laser intensities, opening a new paradigm in strong-field physics experiments. High electron energies exceeding the ponderomotive energy in the incident light field by several orders of magnitude were achieved in an all-plasmonic electron acceleration scheme within the closest nanoscale proximity of the metal film. These results were confirmed by a quantum mechanical model of the light-matter interaction process leading to the same qualitative conclusions. The favourable scaling of γ leads to even lower intensities for strong-field physics paving the way toward strong-field THz science, as well. The observed increase of the kinetic energy of strong-field electrons further toward the infrared is expected to be limited by the quenching of their quiver motion[12]. We also do not expect to achieve more favorable strong-field emission results for long-wavelength sources when using localized plasmons on metal nanoparticles instead of propagating surface plasmons on thin films. The large negative permittivity of noble metals in the mid-IR does not allow the generation of localized plasmons on sub-wavelength-sized nanoparticles (unlike in the visible wavelength range), therefore, large field enhancement factors can equally well be provided by propagating surface plasmons.

Our experiments open the doorway to strong-field physics studies with low laser intensities with simple femtosecond laser oscillators instead of the complex amplifier architectures used for such experiments currently. Moreover, plasmonic field enhancement, together with the strong electric field localization, enable investigations in the nanoscale vicinity of plasmonic structures. By tailoring these nanostructures, ultrafast electron processes can be exploited for a number of applications including extreme ultraviolet light generation[16] and the construction of nanostructured plasmonic photocathodes[32,33].

Methods

The laser source is described in detail in Ref. 22. We measured a pulse duration of 90 fs with maximum pulse energies of 3.8 μJ at a central wavelength of 3.1 μm and a repetition rate of 100 kHz. These pulses were focused onto the hypotenuse face of a right-angle CaF_2 prism where they generated propagating surface plasmons on a 15 nm thick gold film in the Kretschmann-Raether surface plasmon coupling configuration[14]. The film thickness chosen maximized light-plasmon coupling at 3.1 μm and focal spot sizes were 870 and 1400 μm diameter (intensity full width at half maximum, FWHM), measured with knife-edge scans at a plane equivalent to that of the thin film. At the peak intensities of <5 GW/cm^2 used in the experiments, we do not observe any laser damage of the thin film or signal degradation.

The optimum surface plasmon coupling angle is identified by precisely rotating the prism and monitoring the disappearance of the specularly reflected light from the gold surface indicating the coupling of the incident light to a propagating surface plasmon mode[14]. We calculate an optimum angle of incidence of 45.1 degrees (at the hypotenuse face of the prism). The calculated surface plasmon resonance curve has a full width at half maximum (FWHM) of 0.5 degrees which is more than twice the half angle of the cone of the focused beam in the experiments. Thus, we do not consider a varying coupling efficiency across the beam profile and typically measured efficiencies better than 80% with the described method. The prism was mounted as the window of a vacuum chamber, therefore, we could readily carry out spectroscopic measurements of the plasmonically photoemitted and photoaccelerated electrons from the film. This was performed with a retarding potential energy analyzer setup with a retardation grid followed by an electron multiplier detector. The detection setup is described in more detail in Ref. 6. The setup was capable of recording electron spectra and integrated total photocurrent.

The quantum mechanical model of the light matter interaction is based on solving the one-dimensional time-dependent Schrödinger equation (1D-TDSE) for a single active electron in a model potential. We employ a narrow, few ångström wide potential well with variable depth to model the metal surface. Depth and width of the well are chosen to match the actual metal thin film parameters. The ground state of the active electron represents the initial state in the metal thin film. The electronic wavefunction is confined by an infinitely high potential on one side and a potential step on the other, representing the metal-vacuum surface barrier. Additionally, we consider an image-force potential that results in a smoother shape of the surface barrier potential. The evanescent part of the electronic wavefunction penetrates into the classically forbidden vacuum region and this behavior allows us to model adequately the rescattering mechanism which is mainly responsible for the high energy region of the photoelectron spectrum. The electronic wavefunction is then time propagated using the Crank-Nicolson approach under the influence of the plasmon enhanced laser field. Finally, the photoelectron spectrum is retrieved using energy analysis techniques (for more details see e.g. Refs. 34–37).

1. Aeschlimann, M. *et al*. Observation of surface enhanced multiphoton photoemission from metal surfaces in the short pulse limit. *J. Chem. Phys.* **102**, 8606 (1995).
2. Tsang, T., Srinivasan-Rao, T. & Fischer, J. Surface-plasmon field-enhanced multiphoton photoelectric emission from metal films. *Phys. Rev. B* **43**, 8870 (1991).
3. Zawadzka, J., Jaroszynski, D. A., Carey, J. J. & Wynne, K. Evanescent-wave acceleration of ultrashort electron pulses. *Appl. Phys. Lett.* **79**, 2130–2132 (2001).
4. Kupersztych, P. J., Monchicourt, P. & Raynaud, M. Ponderomotive acceleration of photoelectrons in surface-plasmon-assisted multiphoton photoelectric emission. *Phys. Rev. Lett.* **86**, 5180–5183 (2001).
5. Irvine, S. E., Dechant, A. & Elezzabi, A. Y. Generation of 0.4-keV Femtosecond Electron Pulses using Impulsively Excited Surface Plasmons. *Phys. Rev. Lett.* **93**, 184801 (2004).
6. Dombi, P. *et al*. Observation of few-cycle, strong-field phenomena in surface plasmon fields. *Opt. Express* **18**, 24206 (2010).
7. Rácz, P. *et al*. Strong-field plasmonic electron acceleration with few-cycle, phase-stabilized laser pulses. *Appl. Phys. Lett.* **98**, 111116 (2011).
8. Schertz, F., Schmelzeisen, M., Kreiter, M., Elmers, H.-J. & Schönhense, G. Field Emission of Electrons Generated by the Near Field of Strongly Coupled Plasmons. *Phys. Rev. Lett.* **108**, 237602 (2012).
9. Nagel, P. M. *et al*. Surface plasmon assisted electron acceleration in photoemission from gold nanopillars. *Chem. Phys.* **414**, 106–111 (2013).
10. Dombi, P. *et al*. Ultrafast strong-field photoemission from plasmonic nanoparticles. *Nano Lett.* **13**, 674–678 (2013).

11. Krüger, M., Schenk, M. & Hommelhoff, P. Attosecond control of electrons emitted from a nanoscale metal tip. *Nature* **475**, 78–81 (2011).
12. Herink, G., Solli, D. R., Gulde, M. & Ropers, C. Field-driven photoemission from nanostructures quenches the quiver motion. *Nature* **483**, 190–193 (2012).
13. Piglosiewicz, B. *et al.* Carrier-envelope phase effects on the strong-field photoemission of electrons from metallic nanostructures. *Nature Phot.* **8**, 37–42 (2014).
14. Raether, H. *Surface Plasmons on Smooth and Rough Surfaces and on Gratings* (Springer, Berlin, 1988).
15. Schuller, J. A. *et al.* Plasmonics for extreme light concentration and manipulation. *Nat. Mater.* **9**, 193−204 (2010).
16. Sivis, M., Duwe, M., Abel, B. & Ropers, C. Extreme-ultraviolet light generation in plasmonic nanostructures. *Nat. Phys.* **9**, 304–309 (2013).
17. Thomas, S., Krüger, M., Förster, M., Schenk, M. & Hommelhoff, P. Probing of Optical Near-Fields by Electron Rescattering on the 1 nm Scale. *Nano Lett.* **13**, 4790–4794 (2013).
18. Keldysh, L. V. Ionization in the field of a strong electromagnetic wave. *Sov. Phys. JETP* **20**, 1307 (1965).
19. Tóth, C., Farkas, G. & Vodopyanov, K. L. Laser-induced electron emission from an Au surface irradiated by single picosecond pulses at $\lambda = 2.94$ μm. The intermediate region between multiphoton and tunneling effects. *Appl. Phys. B.* **53**, 221–225 (1991).
20. Dombi, P. & Rácz, P. Ultrafast monoenergetic electron source by optical waveform control of surface plasmons. *Opt. Express* **16**, 2887–2893 (2008).
21. Dombi, P., Rácz, P. & Bódi, B. Surface plasmon enhanced electron acceleration with few-cycle laser pulses. *Laser Part. Beams* **27**, 291–296 (2009).
22. Chalus, O., Thai, A., Bates, P. K. & Biegert, J. Six-cycle mid-infrared source with 3.8 μJ at 100 kHz. *Opt. Lett.* **35**, 3204–3206 (2010).
23. Bormann, R., Gulde, M., Weismann, A., Yalunin, S. V. & Ropers, C. Tip-Enhanced Strong-Field Photoemission. *Phys. Rev. Lett.* **105**, 147601 (2010).
24. Irvine, S. E. & Elezzabi, A. Y. Surface-plasmon-based electron acceleration. *Phys. Rev. A* **73**, 013815 (2006).
25. Farkas, G., Tóth, C. & Köházi-Kis, A. Above-threshold multiphoton photoelectric effect of a gold surface. *Opt. Eng.* **32**, 2476–2480 (1993).
26. Paulus, G. G., Becker, W., Nicklich, W. & Walther, H. Rescattering effects in above-threshold ionization: a classical model. *J. Phys. B: At. Mol. Opt. Phys.* **27**, L703–L708 (1994).
27. Walker, B., Sheehy, B., Kulander, K. C. & DiMauro, L. F. Elastic Rescattering in the Strong Field Tunneling Limit. *Phys. Rev. Lett.* **77**, 5031–5034 (1996).
28. Krause, J. L., Schafer, K. J. & Kulander, K. C. High-Order Harmonic Generation from Atoms and Ions in the High Intensity Regime. *Phys. Rev. Lett.* **68**, 24 (1992).
29. Corkum, P. Plasma Perspective on Strong-Field Multiphoton Ionization. *Phys. Rev. Lett.* **71**, 13 (1993).
30. Krüger, M., Schenk, M., Föster, M. & Hommelhoff, P. Attosecond physics in photoemission from a metal nanotip. *J. Phys. B* **45**, 074006 (2012).
31. Wachter, G. *et al.* Electron rescattering at metal nanotips induced by ultrashort laser pulses. *Phys. Rev. B* **86**, 035402 (2012).
32. Graves, W. S., Kartner, F. X., Moncton, D. E. & Piot, P. Intense Superradiant X Rays from a Compact Source Using a Nanocathode Array and Emittance Exchange. *Phys. Rev. Lett.* **108**, 263904 (2012).
33. Li, R. K. *et al.* Surface-Plasmon Resonance-Enhanced Multiphoton Emission of High-Brightness Electron Beams from a Nanostructured Copper Cathode. *Phys. Rev. Lett.* **110**, 074801 (2013).
34. Schafer, K. J. The energy analysis of time-dependent numerical wave functions. *Comp. Phys. Comm.* **63**, 427 (1991).
35. Schafer, K. J. & Kulander, K. C. High Harmonic Generation from Ultrafast Pump Lasers. *Phys. Rev. Lett.* **78**, 638 (1997).
36. Ciappina, M. F. *et al.* Above-threshold ionization by few-cycle spatially inhomogeneous fields. *Phys. Rev. A* **86**, 023413 (2012).
37. Ciappina, M. F. *et al.* High energy photoelectron emission from gases using plasmonic enhanced near-fields. *Laser Phys. Lett.* **10**, 105302 (2013).

Acknowledgments

P.R. and P.D. were supported by the Hungarian Academy of Sciences (Postdoctoral Fellowship and "Lendület" Grant, respectively). The authors wish to thank Győző Farkas and Norbert Kroó for fruitful discussions. This research was made possible in part by a grant of high performance computing resources and technical support from the Alabama Supercomputer Authority. In addition, we acknowledge partial support from the Hungarian Scientific Research Fund (projects 109257 and 109472), the Max Planck Society (Partner Group Program), the Spanish Ministerio De Economia Y Competitividad (MINECO) through its Consolider Program (SAUUL-CSD 2007-00013), "Plan Nacional" (FIS2011-30465-C02-01) and the Catalan Agencia de Gestió d'Ajuts Universitaris i de Recerça (AGAUR) with SGR 2009-2013. This research has been partially supported by Fundació Cellex Barcelona, LASERLAB-EUROPE grant agreement 228334 and COST Actions MP1203 and MP1302.

Author contributions

S.M.T. and P.R. contributed equally to this work. S.M.T., P.R., A.T., J.F. and P.D. carried out the experiments. S.M.T., P.R. and P.D. analysed the data and prepared the figures in the main manuscript. M.F.C. and J.A.P.-H. performed the numerical simulations. L.V. carried out the space charge calculations, wrote the Supplementary Information text and prepared the figures in it. S.M.T. and P.D. wrote the main manuscript text. J.B., A.Y.E. and P.D. supervised the project. All authors reviewed the manuscript.

Additional information

Supplementary information accompanies this paper at http://www.nature.com/scientificreports

Competing financial interests: The authors declare no competing financial interests.

How to cite this article: Teichmann, S.M. *et al.* Strong-field plasmonic photoemission in the mid-IR at <1 GW/cm^2 intensity. *Sci. Rep.* **5**, 7584; DOI:10.1038/srep07584 (2015).